

High carbon yielding and melt processable bis-*ortho*-diynylarene (BODA)-derived resins for rapid processing of dense carbon/carbon composites

Ernesto I. Borrego ^{a,c}, Sumudu Athukorale ^a, Saidulu Gorla ^a, Alison K. Duckworth ^a, Myles Baker ^d, Jonathan Rosales ^d, William W. Johnson ^{a,b}, Santanu Kundu ^{b,c}, Hossein Toghiani ^{b,c}, Behzad Farajidizaji ^a, Charles U. Pittman Jr. ^{a,c}, Dennis W. Smith Jr. ^{a,c,*}

^a Department of Chemistry, Mississippi State University, Mississippi State, MS, 39762, USA

^b The Dave C. Swalm School of Chemical Engineering, Mississippi State University, Mississippi State, MS, 39762, USA

^c MSU Advanced Composites Institute, Mississippi State University, Mississippi State, MS, 39762, USA

^d M4 Aerospace Engineering Inc, 4020 Long Beach Blvd #2, Long Beach, CA, 9087, USA

ARTICLE INFO

Keywords:

Enediyne
Bis-*ortho*-diynylarene
BODA
Carbon/carbon composites
Bergman cyclization

ABSTRACT

Bis-*ortho*-diynylarene (BODA)-derived resins undergo thermal, radical-mediated Bergman cyclization to predominately naphthalene diradicals which propagate in a stepwise fashion to highly branched processable intermediates that are amenable to current composite fabrication techniques prior to network cure and subsequent carbonization. Post-carbonization analysis reveals significantly higher density and consolidation in the BODA-derived carbon/carbon (C/C) over existing phenolic-based C/Cs without the need for arduous, multiple infusion and carbonization steps. The modular BODA approach combines and controls: (1) variable melt processability dictated by terminal or spacer group substitution, (2) mild cure kinetics via a non-autocatalytic reaction, (3) high carbon yield (>80%) to provide relatively dense (~1.55 g/cm³) C/C substrates after a single carbonization at 1000 °C, and (4) remarkable efficiencies that allow fast carbonization ramp rates (10 °C/min) while maintaining high density. Isothermal DSC kinetics, monomer melt stability in air, order/disorder characterization by Raman and WAXS, resin processing under selected air environments, and fractured cross-section analyses of C/C composites by SEM is discussed.

1. Introduction

Carbon fiber-reinforced carbon matrix (C/C) composites have been studied and commercialized for over half a century, yet today the C/C industry remains plagued by long manufacturing cycles due to the utilization of decades old carbon matrix precursors for their fabrication. These standard precursors including, for example, phenolic resins and mesophase pitches are cheap but require multiple slow re-infusion/re-densification cycles and/or high-pressure processes. Processing from these precursors produces property-killing voids and weak interfaces in the laminate due to their polycondensation chemistry and low carbon yield (phenolic resin) or poor processability and reproducibility (pitches) [1–4]. To achieve consolidated C/C composite laminates with reliable thermal and mechanical properties at reasonable overall costs, a single step infusion/carbonization process utilizing a melt-processable,

high carbon yield polyaddition resin is desired.

Synthetic targets with a high theoretical carbon yield include polycyclic aromatic hydrocarbons (PAHs) represented best by various mesophase pitch mixtures [1,2]. Aromatics with additional reactive unsaturation have been promising because of their high mass retention after carbonization at 800–1000 °C. Poly(phenylacetylene) (PPA) derivatives (Fig. 1a) [6], mixed propargyl and allyl-containing cyclopentadiene resins (Fig. 1b) [7], polarylacetylenes (PAA)s (Fig. 1c) [8, 9], perfluoropyridine-derived polyarylenes [10], and poly(*p*-phenylenevinylene) (PPVs) [11] are among the most high yielding carbon precursors of this class. The alkyne rich resins in particular (Fig. 1a–c) consistently exhibit the highest carbon yields [6,7,10,12–18], however the same rigid aromatic and alkyne motifs that impart high carbon yield also inherently contribute to poor processability.

In addition, the polymerization and side reactions in these systems

* Corresponding author. Chemistry Department, Department of Chemistry, Mississippi State University, MS State, MS, 39762, USA.

E-mail address: dsmith@chemistry.msstate.edu (D.W. Smith).

may not be amenable to large scale processes. For example, many PPA derivatives are air and light sensitive, which limits shelf life [6]. The PAA class are difficult to process because of their extremely exothermic cures and low C/C composite interlaminar shear strengths [8,9]. Furthermore, PAAs are often prepared with catalysts or initiators that remain as mobile impurities in the final cross-linked polymer and later in the C/C composite part [6,9,19]. Therefore, regardless of the high initial carbon composition, the specific molecular architecture of the carbon precursor is vital to achieving a combination of properties appropriate for this application which include melt/solution processability, air stability, controlled cure kinetics, high carbon yield, long shelf life, high carbon crystallinity, high thermal mechanical properties and reproducibility.

Herein we present a synthetic platform based on bis-*ortho*-diynylarene (BODA) monomers as a new class of carbon precursor resin that can be melt-infused into a carbon fiber fabric, cured, and pyrolyzed to a relatively dense (1.55 g/cm^3) C/C composite after a single carbonization cycle at $1000\text{--}1500^\circ\text{C}$. BODA monomers convert to polynaphthalene networks via a thermal-initiated, reagent-free Bergman cyclization (Fig. 1d) [20–22]. Its performance and processing parameters can be expanded by proper formulation with ODA functional co-monomers, and other reactive diluents or additives. Furthermore, BODA-type materials as an unformulated base can be synthesized from commercially available bisphenols by three well-established reactions (Fig. 2) [23]. The Bergman cyclization (B.C.) is a unique aromatization reaction that has been underutilized for the synthesis of advanced materials, but has been intensely studied since the 1970s and is well defined [20,21,24,25]. The reaction proceeds free of catalysts or reagents so the resulting polymer is free of mobile impurities such as metal ions which may cause degradation in application.

Previous work has reproducibly demonstrated the high carbon yields [26,27] and exceptional melt/solution processability of these BODA-derived resins [23]. The BODA strategy has been utilized to fabricate solid and hollow carbon fibers [28], carbon-based photonic

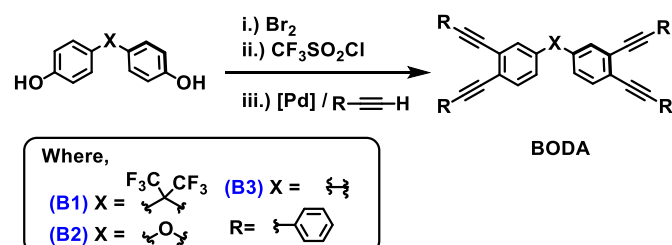


Fig. 2. A general synthetic approach to BODA monomers, wherein X- and R-groups represent synthetic handles that can be substituted for custom property tuning. Experiments herein contain examples of phenyl-terminated R-groups only (B1–B3).

crystals [29], and other carbonaceous materials [22,27]. These proven qualities formed the impetus for further investigation of its capacity as a revolutionary carbon matrix precursor for C/C applications.

2. Experimental

2.1. Materials

$[\text{P}(\text{Ph})_3]_2\text{PdCl}_2$ was purchased from Sigma Aldrich, 4,4'-bisphenol from Key Organics, trifluoromethanesulfonyl chloride from Synquest, *N,N*-dimethylformamide (anhydrous, amine free) from Alfa Aesar, and dichloromethane (CH_2Cl_2) from Fisher Chemical. Phenylacetylene, 4,4'-dihydroxyphenyl ether, 4,4'-hexafluoroisopropyl-bisphenol, and iron (powder, ~325 mesh, reduced) were all purchased from AK Scientific. Trifluoromethanesulfonyl anhydride, glacial acetic acid (HOAc), triethylamine (99.7%, extra pure), bromine, and CuI were all purchased from Oakwood Chemical. Synthesis of the BODA monomers was carried out using the above mentioned chemicals as received without further purification and according to a previous literature procedure [23]. The resole-type phenolic resin (PLENCO 14670) used for our control

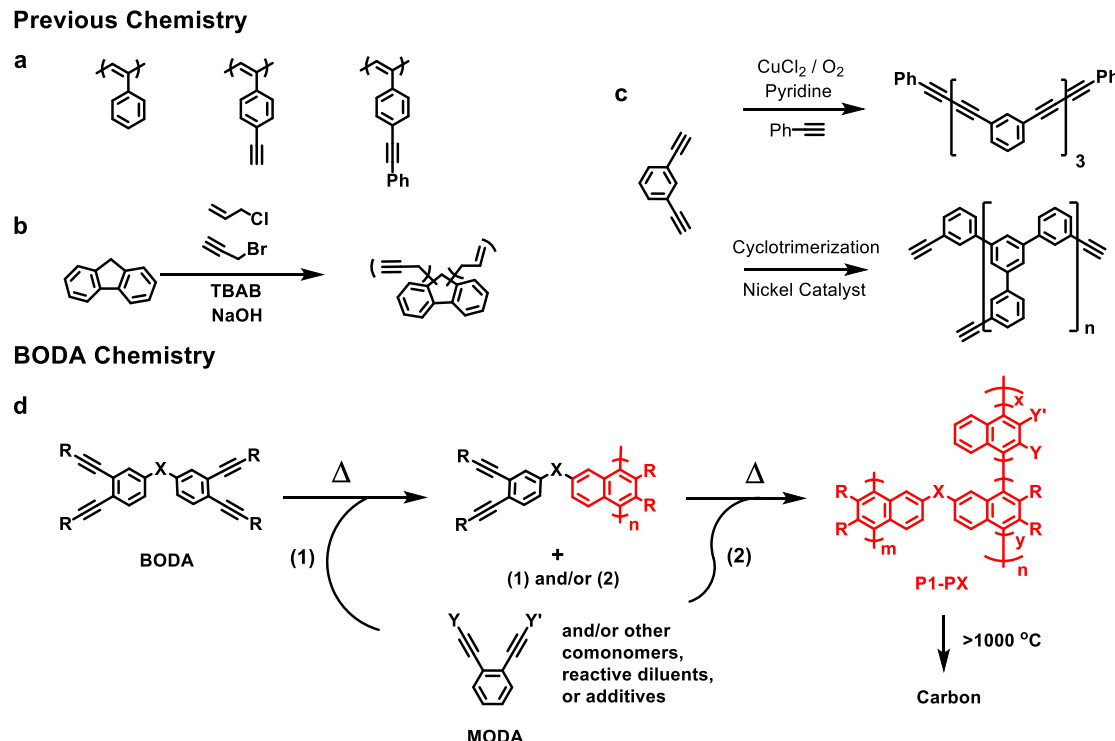


Fig. 1. Thermally curable poly(phenylacetylene) (PPA) derivatives (a), mixed propargyl/allyl cyclopentadienes (b), polyarylacetylene (PAA) resins from *m*-diethylnylbenzene (c) and general polymerization, crosslinking, and carbonization of bis-*ortho*-diynylarene (BODA) monomers with or without comonomers or additives before (1) or after (2) B-staging of the resin (d).

experiments was donated by PLENCO. The T300 carbon fibers from Toray were donated by the MSU Advanced Composite Institute (ACI). T700S-12K 8-HS carbon fiber weaves were provided by M4 Aerospace Engineering and are from Toray. The (97x16 × 10mm) porcelain combustion boats used for small-scale carbonization experiments were purchased from United Scientific Supplies, Inc.

2.2. Synthesis of monomers

2.2.1. Synthesis of B1–B3

The synthesis of BODA monomers **B1–B3** was carried out according to previous literature procedures [23]. Although well established, BODA monomers serve as the base material in multi-component custom resin formulations and B-staged intermediates for carbon/carbon composite applications under commercial development by Hand Technologies, LLC (Starkville, MS).

2.3. Monomer and polymer characterization

Fourier Transform Infrared Spectroscopy (FTIR) experiments were conducted using an Agilent Cary 630 spectrophotometer with a diamond crystal ATR sample head scanning between the wavelengths of 4000 to 400 cm⁻¹ with resolution of 2 cm⁻¹. Nuclear magnetic resonance (NMR) experiments (¹H, ¹⁹F, ¹³C) were performed on a Bruker AVANCE III 500 MHz instrument. Chloroform-d (CDCl₃) was used as a solvent for NMR experiments, and all chemical shifts are reported in parts per million (δ ppm). Differential scanning calorimetric (DSC) experiments were conducted using a TA Q20 V4 DSC instrument. Approximately, 5–9 mg of the monomer or polymer was placed in a TA low-mass aluminum pan and sealed. Heating and cooling cycles were performed from 0 to 400 °C at a scanning rate of 10 °C/min, unless stated otherwise. Between the cycles, the pans were isothermally held at 400 °C and at 0 °C for 1 min, unless stated otherwise. Thermal decomposition data was collected on small samples (5–10 mg) using a TA Q50 V20 Thermogravimetric Analyzer (TGA) instrument over the temperature range of 30–1000 °C, at a heating rate of 10 °C/min, unless otherwise stated. The experiments were carried out under both nitrogen and air, and TA universal analyses software was used to analyze the decomposition patterns. Melt properties of BODA-derived resins were obtained using a parallel plate experiment on a Discovery HP-2 Hybrid Rheometer. Approximately 100–300 mg of solo BODA resins were added to the plate accessory at 180 °C, melted, and mixed to remove any trapped air bubbles and ensure full plate coverage. Low shear rates (0.1 s⁻¹) were used.

2.4. Thermal cure of resins

As shown here and in previous reports [22,27], polymerization and thermoset cure is performed from 200 to 400 °C at 1 °C/min. Very slow decomposition (<1%/h) occurs at 400 °C (isothermal) for BODA **B1–B3**, and is chosen as the maximum cure temperature prior to carbonization. For comparison, phenolic resins cure at 80–100 °C (1 °C/min) [30,31] and begin to decompose at temperatures above 300 °C [32]. The phenolic resin used for comparison in this study was cured at 80 °C for 3 h, similar to recent literature [31].

2.5. Thermal conversion of resins to amorphous carbon

Each of the BODA- and phenolic-derived thermosets were thermally converted to carbon at carbonization rates between 1, 3, 5, and 10 °C/min under an inert atmosphere (N₂ or Ar, at flow rates of 50 or 100 mL/min) to 1000 °C. Selected samples, as noted in the text or figures below, were heated to 1200 or 1500 °C. Comparisons between BODA- and phenolic-derived monolithic carbons and their C/C composites were determined by carbonization under the same conditions: carbonization rate, gas, flow rate of gas, final carbonization temperature, dwell time at the final temperature, and % fiber volume.

2.6. Fabrication of C/C composites

C/C composites reported here were targeted to have a 60% fiber volume to normalize fiber-dominant properties. To fabricate a 6"x6"x0.2" panel with a total volume of 117.98 cm³ C/C, 124 g T300 ($d_{T300} = 1.76 \text{ g/cm}^3$) is required. The remaining 40% (v) would be carbon-derived from resin. This amount is 75.45 g of amorphous carbon when using **B3** ($d_{B3\text{-Carbon}} \sim 1.50 \text{ g/cm}^3$). Therefore, resin quantities added to each panel would be varied according to their corresponding carbon yields and weight losses over curing. For example, solo BODA-Biphenyl (**B3**) with no other additives or comonomers has a weight loss of ~2% during its cure and an ~83% carbon yield. This would require 92.76 g of **B3**-derived resin to result in the 75.45 g or 40% by vol carbon matrix. Though a 60% fiber volume was targeted according to these calculations, the compositions of coupons herein are reported in wt % hereafter.

Thin C/C coupons from BODA or phenolic precursors were fabricated by hand lay-up into a ceramic boat. All C/C composites reported here were made with heat-treated (10 °C/min, 1000 °C, 2 h, 50 mL/min Ar) T300 carbon fibers. Once the prepgs were made and cured according to their respective chemistry they were carbonized at 1 °C/min to 1000 °C with a 60 min dwell time in a tube furnace under 100 mL/min Ar flow.

Due to the differences between the resol and BODA-derived resins in physical state at room temperature, their respective prepgs were prepared by different impregnation methods. C/C composites made using resol (PLENCO 14670) were prepared by first adding liquid resol solution to a preheat-treated T300 fabric preform (7 plies, quasi-isotropic) and allowing it to infuse (ambient pressure) through the thickness. In all cases, before impregnation, the resol resin was degassed under vacuum for 30 min or until all observable gas bubbles were removed. Intermediate pre-cured samples were prepared and placed under Ar at 100 mL/min for periods of 60 min or more before curing or carbonizing. The phenolic-prepg coupons were carefully compacted prior to cure and degassed to squeeze out any trapped air bubbles and aid bonding and lamination between plies. The resole-derived samples were then placed in a tube furnace and cured under Ar.

BODA-derived C/C composites were prepared by a powder-melt impregnation which involved adding BODA powder to a carbon fiber fabric preform (T300 or T700S-12K). In each case, the powder was carefully distributed and packed between laminae before being melt impregnated (ambient pressure) in a furnace at 180 °C for 30 min under Ar flow. For thin coupons that were compared against the resol-derived C/C, pre-heated T300 fibers were used (using 7 plies in a quasi-isotropic stacking sequence). For thicker coupons, the T700S-12k 8-HS weave was used (12 plies in a 0/60/-60 stacking sequence, Table 1) and the fiber preforms were melt-impregnated via vacuum bag-assisted infiltration.

Table 1
Layer-by-layer assembly of high temperature vacuum bag assisted-infiltration.

Layer	Ply ID	Material	Angle
1	–	Aluminum Plate	–
2	–	Red Release Tape	–
3	–	Armalon	–
4	–	BODA	–
5	P01	TORAY T700S-12K	0/90
6	–	BODA	–
7	P02	TORAY T700S-12K	60/30
8	–	BODA	–
9	P03	TORAY T700S-12K	–60/-30
69	–	BODA	–
70	–	Armalon	–
71	–	Polyimide Release Film	–
72	–	Fiberglass Breather	–
73	–	Caul Plate	–
74	–	Polyimide Bagging Film	–

2.7. Glassy carbon and C/C composite characterization

A JEOL JSM-6500F field emission scanning electron microscope (SEM) was used for the cross-sectional micrographs and fractographic analysis of the C/C composites presented herein. All samples were coated with 15 nm of Pt to provide sufficient conductivity for imaging. Five samples were analyzed for each BODA- and phenolic resin-derived C/C coupon. With regard to the sample size/selection for studies on the effect of cure/carbonization schedules on carbon microstructures, three different cross section surfaces were analyzed per sample and two samples per entry were studied. Micrographs shown in all the figures below were chosen on the basis that they were widely representative of the overall qualitative results observed in the sample set (e.g. surface roughness, porosity, delamination, etc.). Electron dispersive X-ray (EDX) spectroscopy was carried out under 15 kV and a working distance less than 10 mm. The Archimedean densities of the carbon materials were obtained via ASTM C 693. A LabRam HR800 confocal Raman microscope equipped with an Olympus 10x objective ($\text{NA} = 0.25$) and a He/Ne laser, with an excitation wavelength of 632 nm, was used for all Raman acquisition. The laser power before the objective was 13 mW and the spectrograph grating was 600 grooves/mm. The acquisition times for all spectra were varied between 10 and 200 s. The Raman shift values were calibrated with a neon lamp. Reflective sample substrate (RSS) slides from Raminесcent, LLC were used for all Raman acquisitions.

3. Results and discussion

3.1. BODA-derived resins and their glassy carbons

The general synthesis of BODA monomers and ODA-functional co-monomers and resins is well established and shown in Fig. 2 [23,27]. The scope of polymerization, network formation, and carbonization has also been enhanced to include resin formulations with and without co-monomers, reactive diluents, or other additives designed for specific process parameters and ultimate C/C properties. Although additives reduce cure time and viscosity for processing, it must be emphasized that rigid BODA monomers (e.g. B1–B3, Fig. 2) alone have relatively wide melt processing windows prior to gelation due to the myriad of branching repeat unit structures possible through the Bergman cyclization (B.C.). For example, the aggressive diradicals can cyclize to form polynaphthalene repeat units (Fig. 3 in blue) with small amounts of benzofulvene units (red) and couple together in a step-wise fashion or undergo chain-initiation to a small degree in certain monomers [33]. The branching and repeat structure “irregularities” greatly enhances the solubility of BODA-derived polymeric intermediates relative to traditional linear polyarylenes with singular identical repeating units, and pre-mature interchain packing prior to vitrification.

As observed by TGA (Fig. 4a) the biphenyl-containing BODA (B3) gave the highest carbon yields of all the BODA-derived resins studied herein (B1–B3, see Fig. 2) and are comparable to mesophase pitches (>80%), claimed to be the highest carbon yielding matrix precursor known for C/C composite fabrication [34]. The carbon yields obtained from the hexafluoro-*i*-propyl- and ether-containing BODAs (B1 and B2, respectively) were lower than B3 and pitch-based materials, yet higher than those observed from phenolic resins (40–60%) [9,35]. We attribute

the observed trend in carbon yields (**B3** > **B2** > **B1**) to their respective homolytic bond energy of the spacer group (X in Fig. 2). Although the exact mechanism of volatile product formation is unknown for these materials, aromatic ring fusion and crosslinking via dehydrogenative aromatization in the biphenyl linkage is known [36]. The carbon yields reported here are obtained according to literature precedence, i.e. reporting the yield after thermoset cure and prior to decomposition. Instructed by the exothermic reaction profile by DSC (Fig. 4b), monomers **B1–B3** were cured by heating to 400 °C. In all cases, **B1–B3** reproducibly loses between 2 and 3% during initial heating up to ca. 200 °C due to volatilization and desorption of organic impurities.

As expected, and in accordance with previous reports [22,27], the T_{onset} is identical for **B1–B3** (~210 °C). This is because the activation energy for the curing mechanism, the Bergman cycloaromatization, is dominated by the terminal *trans*-alkyne distance [37,38] and each monomer is functionalized with the same phenyl moiety (same steric repulsion) on the terminal acetylenes (defined as R in Fig. 2). Monomer **B2** has the largest processing window from pure monomer, because of its low melting point at 105 °C. The hexafluoropropyl and ether spacer groups provide a greater degree of freedom about the core phenyl rings, contributing to the lower melting temperature for **B1** ($T_m = 170$ °C) and **B2** to have vs than **B3** ($T_m = 180$ °C), which has a high degree of rigidity and π - π stacking.

Crystallinity in the resulting BODA-derived glassy carbons was estimated by a standard Raman technique [39]. Here, the ratio of the intensity of Raman signals corresponding to turbostratic or disordered carbon (D) and graphitic (G) phases are taken from a baseline corrected spectra (Fig. 4c). The ratio (I_D/I_G) is commonly reported as measure of crystallinity. These trends were corroborated with powder XRD data (Fig. 4d). Interestingly, there is an apparent correlation between the initial crystallinity of the monomer [40] and the resulting crystallinity of the glassy carbon produced after a non-oxidative pyrolysis at 1000 °C. Similar phenomena can be seen with traditionally used carbon matrix precursors. For example, mesophase pitches tend to yield more graphitic carbons than phenolic resins, however the BODA approach provides modular synthetic handles that can be varied (e.g. X spacers and terminal acetylene R groups, Fig. 2) to offer potential control of evolving carbon structure and ultimate properties. Such control is beneficial in the design of new carbon matrix precursors. Crystalline carbon matrices are often desirable for C/C composites because higher thermal conductivities can be achieved, which ultimately helps in dissipating heat [41].

3.2. Melt processing and curing of BODA-derived resins

Concerns exist around using alkyne-based chemistry which cure via highly exothermic processes that could lead to uncontrolled runaway reactions [8]. The well-defined and controlled Bergman cyclization (B.C.) mechanism enjoyed by BODA polymerization precludes this issue. Isothermal DSC kinetics reveal that the exothermic B.C. for BODA-derived resins proceeds via a non-autocatalytic reaction (Fig. 5a) with the maximum heat evolution occurring upon reaching the dwell temperature. After such time, no additional heat is detected to mark the occurrence of a sustained reaction. These types of reactions can be modeled by n th order kinetics [42,43], i.e. their conversion is

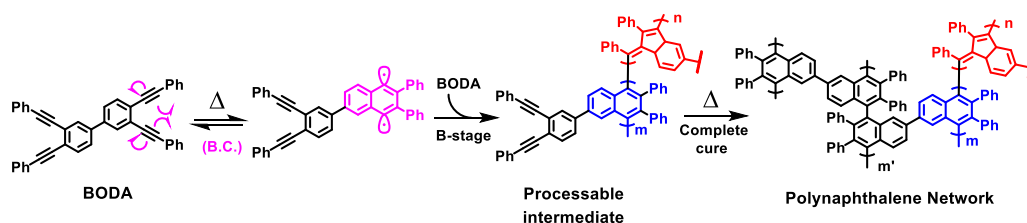


Fig. 3. Schematic representation of B-staging and complete cure of BODA (B3) via a thermal-initiated, catalyst-free Bergman cyclization where $m \gg n$.

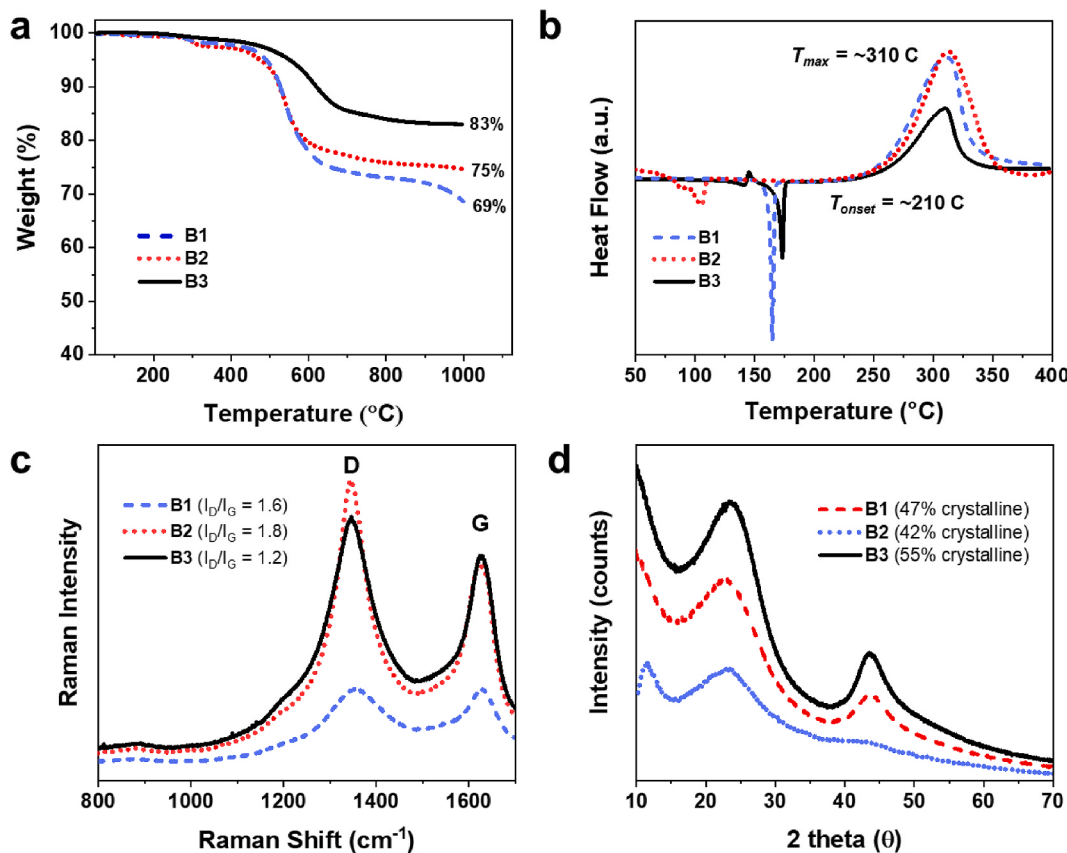


Fig. 4. TGA of **B1–B3** after DSC cure to 400 °C (a) and DSC of BODA monomers **B1–B3** (b), both ramped at 10 °C/min under 50 mL/min of N₂. Raman characterization (c) and p-XRD (d) of the **B1–B3**-derived glassy carbons after carbonization in Ar at 1000 °C, with a ramp rate of 10 °C/min.

temperature dependent and therefore runaway reactions would not be expected during composite fabrication. This is further supported by isothermal DMA studies (parallel plate rheometer), which show no changes in modulus occurring after heating (isothermal) above the T_{onset} measured by DSC (Fig. 5b). Furthermore, non-isothermal DSC analysis reveals the exothermic reaction to release ca. 700 J/g for **B1–B3**. Therefore, the expected heat release from a test panel with the dimensions (6"×6"x0.2") and a percent fiber volume of 60% would be approximately 63.6 kJ. The T300 carbon fiber, having a large surface area contact with the resin and a transverse thermal conductivity of 0.105 J/cm•s °C, will presumably absorb most of the energy released over the cure schedule. Based on the percent fiber volume and density of T300 carbon fibers, each panel of such dimensions would contain 124 g of T300 carbon fiber. The carbon fibers have a large heat capacity ($C_p = 794.96 \text{ J/g} \cdot ^\circ\text{C}$) and will therefore require ~98 kJ to be heated a single degree Celsius; thus a maximum increase in temperature of 0.64 °C can occur during the curing schedule of this system (6"×6"x0.2"). Unlike similar analogs which have high carbon yields, the BODA materials presented herein, to our knowledge, are not subject to uncatalyzed [44] runaway reactions that make their processing difficult or cause highly exothermic events that would be a fire hazard at large scale.

Using the isothermal DSC data generated (Fig. 5a), it was possible to extrapolate the conversion as a function of time and temperature (Fig. 5c). Conversion was calculated using the general rate equation (1) that pertains to *n*th-order kinetics.

$$\frac{d\alpha}{dt} = (dH/dt)/\Delta H_{tot} = k(T)[1 - \alpha]^n \quad (1)$$

Here, $d\alpha/dt$ is the rate of reaction, dH/dt is the heat flow, ΔH_{tot} is the total heat released, $k(T)$ is the rate constant at a specific temperature, n is the reaction order and α is the fractional conversion which could be determined via the following expression:

$$\alpha(T, t) = \frac{1}{\Delta H_{tot}} \int_0^t (dH/dt) dt = \frac{\Delta H_t}{\Delta H_{tot}} \quad (2)$$

The total heat released, ΔH_{tot} , is equal to the sum of the heat released after isothermal hold for a specific time (ΔH_t) and the residual heat released after being cooled and then reheated to 400 °C at 10 °C/min (ΔH_{res}). The data obtained from measuring the conversion as a function of temperature/time (Fig. 5c) and temperature/heating rate (Fig. 5d), guided the design of a proper cure schedule following impregnation at 180 °C.

Surprisingly, the molecular structure, polymerization profile, and carbon yield did not significantly change when processed under air (Fig. 6). After melting **B3** in air isothermally at 180 °C for 3 h, comparative ¹H NMR spectra of **B3** before and after melting under these conditions revealed no observable changes in chemical shift, multiplicity, or peak integrations of the peaks corresponding to the protons on **B3** (Fig. 6a). Furthermore, DSC investigations (Fig. 6b) demonstrated similar results, where a nearly identical exothermic profile was observed for **B3** when cured either under air or under N₂ flow, using the same conditions (ramp rate, final temperature, dwell times, etc.). The most notable deviation was observed around 350 °C in the form of a shoulder exotherm of unknown origin yet may be due to O₂-assisted dehydrogenative aromatization. Following these DSC studies (N₂ and air cured), each **B3**-thermoset was carbonized at 1000 °C under 50 mL/min of N₂ in the TGA (Fig. 6c). The carbon yields for the **B3**-derived thermoset increased when cured in air relative to a cure in N₂.

Air-mediated aromatic annulation or oxidative “stabilization” are utilized in the carbon fiber industry to increase carbon yield in the same manner [45]. Investigations were undertaken to identify the maximum carbon yield attainable by these means. After a complete cure at 400 °C

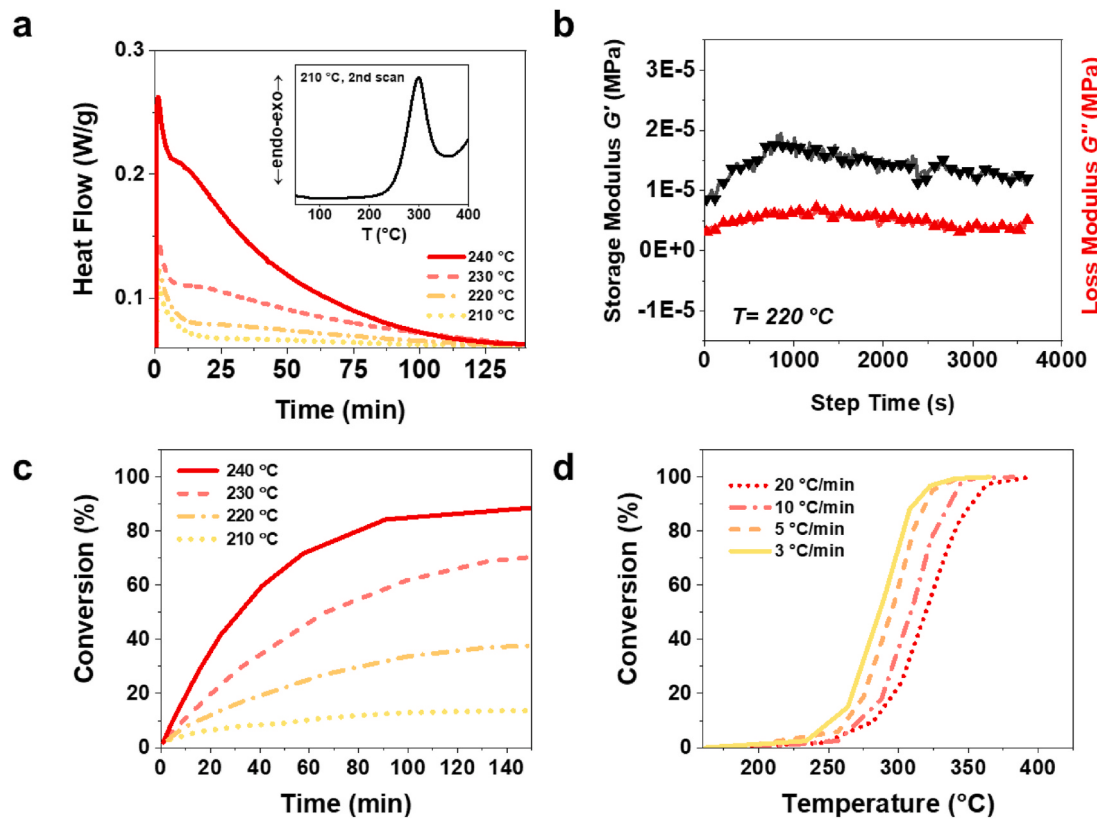


Fig. 5. Isothermal DSC for B3 at various temperatures with dynamic scan (inset, after the 210 °C isothermal sample) (a). Isothermal DMA at 220 °C (b). Experimental conversion as a function of time and temperature, extrapolated from isothermal DSC (c). Experimental conversion as a function of temperature and heating rate, extrapolated from dynamic DSC using the Borchardt and Daniels approach (d).

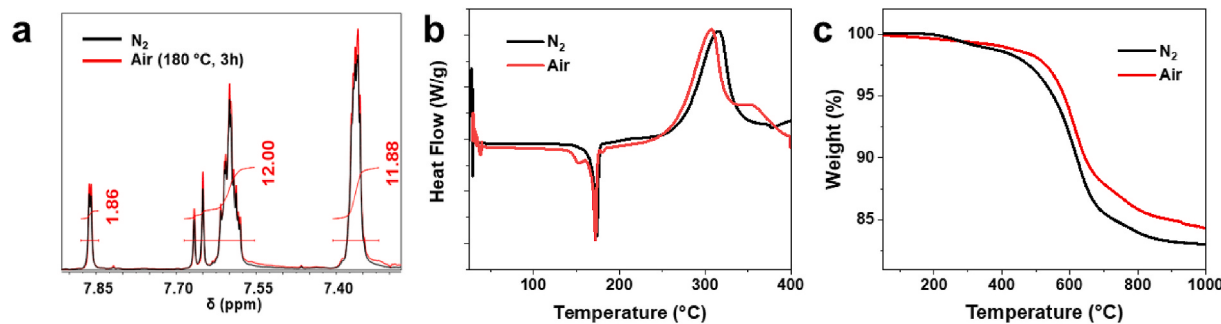


Fig. 6. Thermal oxidative stability of B3. Superimposed ¹H NMR spectra before and after heating B3 at 180 °C in air for 3 h (a). DSC curing profiles (10 °C/min) of B3 under N₂ and air (b). Carbonization by TGA to 1000 °C (10 °C/min in N₂) after DSC cure of B3 under N₂ and air flow (c).

(Fig. 7a), a B3-derived thermoset was pyrolyzed in air to determine the appropriate temperature region to carry out the oxidative studies (Fig. 7b). To this end, oxidative soaking experiments were conducted at 300, 400, and 500 °C each with multiple dwell times (30, 60, and 180 min, Table 2). The weight loss, if any, during the oxidative soaking was recorded (Fig. 7c) and considered when measuring the effect of an oxidative post-cure on the carbon yield. After the oxidative soak, samples were carbonized under N₂ to observe any changes in carbon yields (Fig. 7d). The weight loss observed, if any, during the additional oxidative soak ($W_{l(OS)}$) was subtracted from its final carbon yield ($C_y(OS)$). The difference between this value and the originally reported carbon yield when no oxidative soaking was attempted ($C_y(NOS)$) gave the total carbon yield increase ($\Delta C_y\%$); see equation (3).

$$\Delta C_y\% = [C_y(OS) - W_{l(OS)}] - C_y(NOS) \quad (3)$$

The largest increase in the carbon yield (~3%) was observed after an

oxidative post-cure treatment at 300 °C for 30 min. As the dwell time is extended for the oxidative soaking, the apparent carbon yields become lower with exception of the 400 °C isothermal series. Higher temperatures favor degradation mechanisms that result in significant weight losses during oxidative soaking and therefore decrease the carbon yield relative to the traditionally single-cured samples. More specifically, temperatures of 500 °C and above oxidize the thermoset too quickly to be considered useful, so dwell times above 30 min at 500 °C were not pursued.

3.3. Kinetic factors affecting BODA-derived glassy carbon properties

One of the drawbacks of processing C/C composites via phenolic resins is the slow cure and carbonization requirements for producing an optimally dense laminate. This is because there is high potential for composite defects/voids involved in the “rapid” processing of C/C

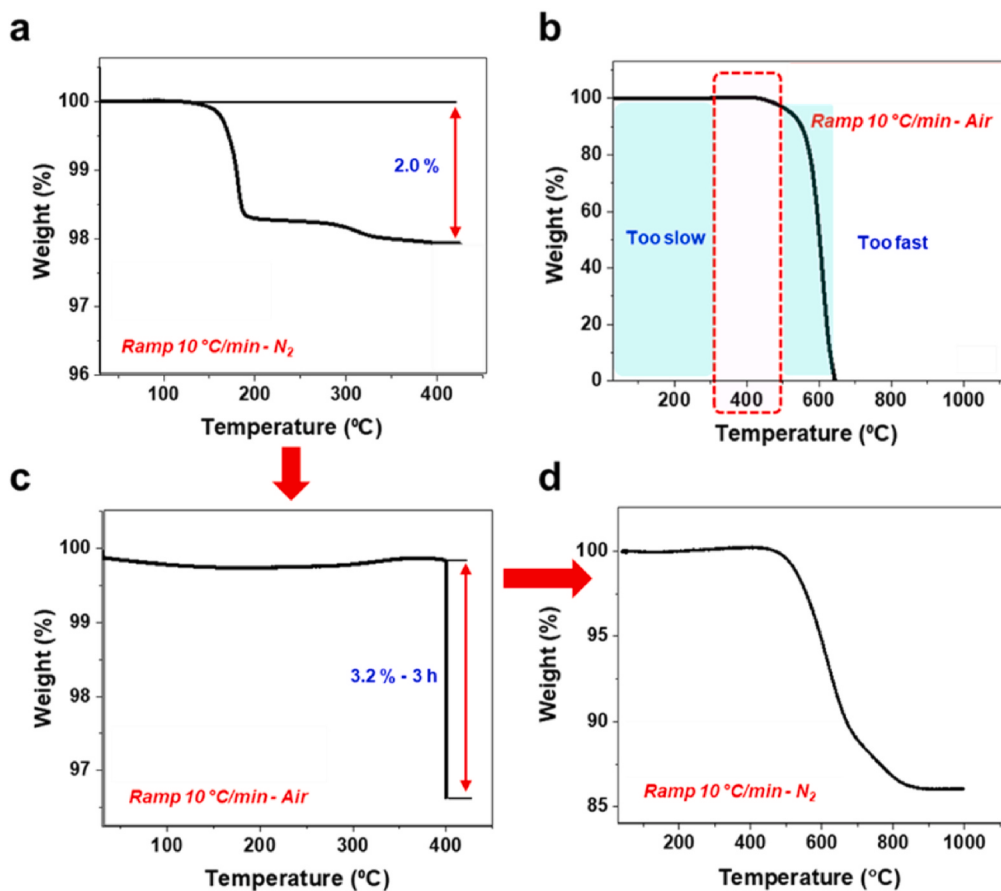


Fig. 7. Oxidative soaking protocol: Initial cure of B3 by TGA to 400 °C in N₂ (a). Carbonization of the cured sample in air (b). Example of an isothermal oxidative soaking experiment in air (c). Carbonization of the oxidatively soaked sample under N₂.

Table 2

Tabulated values from oxidative soaking experiments on B3, after being cured at 400 °C.

Temperature, in air	Dwell time (h)	Wt. loss (%) ^a	Carbon yield (%)	Total Carbon Yield Increase (%) ^b
No Post-Cure	–	–	83.0	–
300 °C	0.5	0	85.6	2.6
	1	0	85.4	2.4
	2	0	85.1	2.1
400 °C	0.5	0.58	85.3	1.72
	1	0.60	86.0	2.40
	3	3.20	85.0	-1.2
500 °C	0	7.93	85.1	-5.83
	0.5	23.76	79.5	-27.26

^a Represents the wt. loss after being held at the corresponding temperature in air, for the corresponding dwell time.

^b The difference between the carbon-yield after post-curing and the original carbon yield without post-cure (B3; 83%) with the weight lost during the post-cure cycle subtracted from that difference; see equation (3).

composites from phenolic resins. While curing they release phenol, formaldehyde, water, and other volatile condensates that can be trapped in the matrix if cured too quickly [32]. Similarly, slow carbonization is required because the resulting thermoset has a high heteroatomic composition and a significant portion of its weight (45–60%) is lost through off-gassing between 600 and 800 °C. These degradation byproducts generate composite-damaging internal stresses such that carbonization rates of 0.5–1 °C/min are often required. Such fabrication processes require longer than a day, without accounting for dwell times and reinfiltration/redensification cycles [5,46,47]. Alternatively, the

BODA materials presented herein, B1–B3, cure without the formation of any volatile condensates, and have a high initial carbon composition. We therefore investigated the effect of the cure and following carbonization ramp rates of the BODA-derived resins on their final glassy carbon properties.

A glassy carbon control sample was prepared by slowly curing and carbonizing B3 at a rate of 1 °C/min. Then its density and degree of crystallinity (I_D/I_G) was measured. To study the isolated effects of the rate of cure and carbonization, only one ramp rate was changed at a time. For example, the cure ramp rate was held at 1 °C/min while the carbonization ramp rate was increased to 5 and 10 °C/min (Table 3, Sample 1 and 2). When the carbonization rate was increased to 5 °C/min and the cure rate held at 1 °C/min, the I_D/I_G value remained the same while a lower density was achieved relative to the control. A drop in both I_D/I_G and density was observed when the carbonization was held at

Table 3

Effect of B3 cure (to 400 °C) & carbonization (400–1000 °C) rate on carbon density and crystallinity.

Sample	Cure rate (°C/min)	Carbonization Rate (°C/min)	Density (g/mL)	I_D/I_G
Control	1	1	1.5 ± 0.01	1.12 ± 0.01
1	1	5	1.46 ± 0.01	1.12 ± 0.01
2	1	10	1.49 ± 0.01	1.15 ± 0.01
3	5	1	1.43 ± 0.01	1.19 ± 0.01
4	10	1	1.31 ± 0.01	1.21 ± 0.01

1 °C/min and the cure ramp rate increased to 5 and 10 °C/min. This indicated that the rate of carbonization has a smaller impact on the final carbon properties than the rate of cure. Therefore, Carbonization of BODA derived resins are likely possible at higher ramp rates than those fabrication schedules typically prescribed today without significantly compromising the quality of the final carbon. This is further demonstrated by the micrographs shown in Fig. 8 and Fig. S1 in the supplemental information.

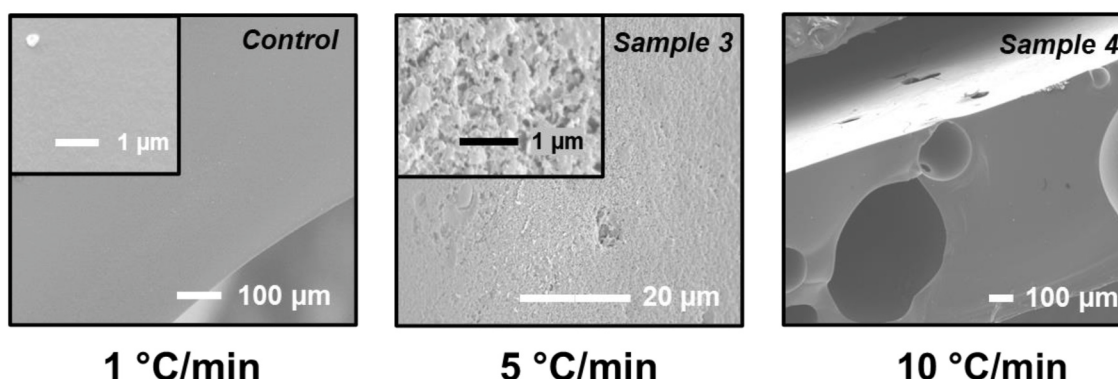
As the cure ramp rate is increased against a constant carbonization ramp rate (1 °C/min), the SEM cross sections of the carbon microstructure are visibly changed. However, in agreement with the density and I_D/I_G measurements, when the carbonization ramp rate is increased against a constant cure ramp rate (1 °C/min) the carbon micrographs remain relatively unchanged (Fig. 8). The SEM images here are largely representative of multiple micrographs taken for each sample at the size scale wherein the first carbon surface features can be observed, if any (e.g. voids, debris from fracture, porosity, etc.). Unsurprisingly, due to the relatively low mass loss upon carbonization in B3 there is no significant porosity generated when the ramp rate at this stage is increased (1, 5, and 10 °C/min). However, there is a larger mass loss observed via TGA in the carbonization region (600–1000 °C) than the curing temperature region (200–400 °C). Therefore, pores generated during high cure ramp rates are likely the result of voids being caught in the matrix as the monomer melts and vitrification ensues. This evolution can be seen in the supplemental information (Fig. S1). Upon curing from 30 to 400 °C, sample 2 (cured at 1 °C/min, see Table 3) shows a rough surface with essentially no pores or void areas that can be observed using an optical microscope up to x50 magnification (Fig. S1a). However, upon curing,

sample 4 (cured 10 °C/min) shows a range of different pore sizes: large (100–200 μm), medium (averaging $\sim 12 \pm 3 \mu\text{m}$), and smaller pores $>1 \mu\text{m}$ (Fig. S1b). These trapped voids remain in the structure even if carbonized slowly. If they are never produced (via slow cure) then a fast carbonization will do little to generate pores afterwards (Figs. S1c–d, and Fig. 8). As commonly understood, a slow cure allows the polymer to organize, stack, and template phase growth that yields a carbon with a higher degree of crystallinity, as indicated by the corresponding I_D/I_G values. The results shown here are different from those expected from phenolic-derived carbon, where fast carbonization ramp rates are typically detrimental to carbon properties and performance. This implies that the BODA approach provides much faster processing times for carbon than those derived from phenol-formaldehyde. First, fewer reinfusions are required using BODA-derived resins. Secondly, the BODA materials have a capacity to be carbonized at much faster carbonization rates without impeding the carbon quality (i.e. uniformity, density, porosity, crystallinity, etc.) [48].

3.4. BODA-derived C/C composite panels

BODA (B1–B3) derived preprints, fabricated via a powder-melt impregnation of a heat-treated (unsized) carbon fiber preform, were carbonized at 1000 °C under 50 mL/min Ar flow to produce dense ($\sim 1.55 \text{ g/mL}$) C/C composites after a single densification (Fig. 9a). The preprints were carbonized with and without a vacuum-assisted apparatus. Thin C/C coupons were fabricated from 2 plies of T300 and B1–B3 without a vacuum bag. On this small scale they demonstrated satisfactory quality, exhibiting a non-porous matrix, minimal carbon fiber

Effect of Cure Ramp Rate



Effect of Carbonization Ramp Rate

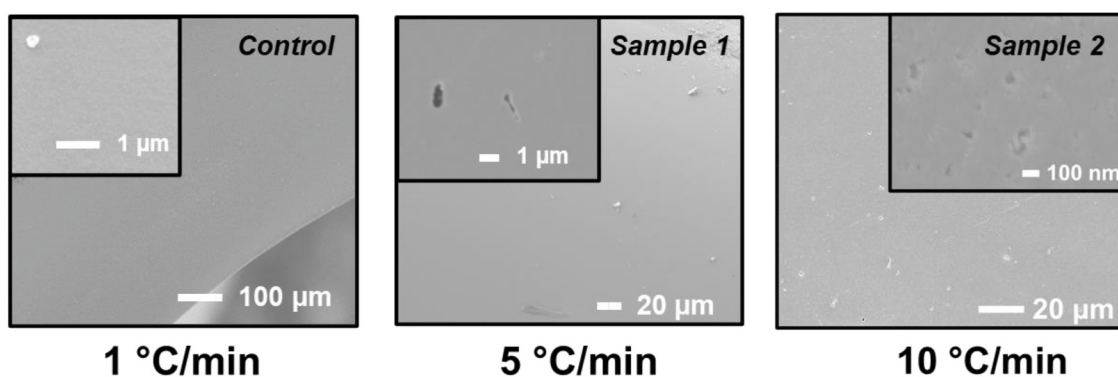


Fig. 8. Effect of cure and carbonization ramp rate on B3-derived carbon micrographs (SEM cross-sections).

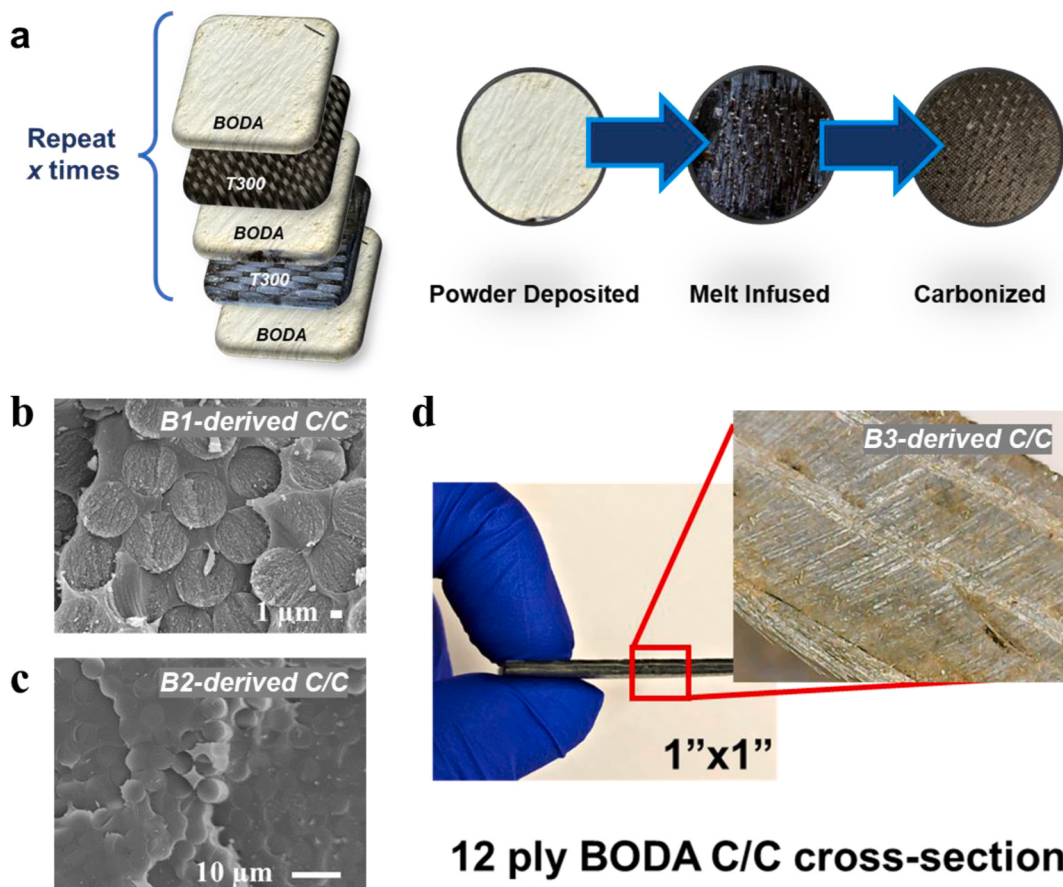


Fig. 9. Composite fabrication using BODA-derived resins, from **B1–B3** (a). SEM cross section of an unpolished fractured **B1**-derived C/C after carbonization at 1500 °C (b), an unpolished, fractured **B2**-derived C/C after carbonization at 1000 °C (c), and a 12-ply **B3**-derived C/C coupon using vacuum bag-assisted infiltration with optical image (inset) of magnified unpolished cross-section (d).

pullout and delamination upon fracturing, and good fiber-matrix bonding (e.g. Fig. 9b and c). Thicker coupons, using 12 plies of a T700S-12k 8-HS weave, were then fabricated through a vacuum-assisted infiltration process to acquire the same results and showed no significant gross porosity even for thicker multi-layer laminates (Fig. 9d). Very little variation in the bonding, delamination and fracture features was observed via SEM or density measurements in a sample set of five of each BODA (**B1–B3**)-derived C/C coupons. Figs. 9 and 10 are widely representative of the results obtained.

A set of 7 ply C/C coupons were fabricated from BODA monomer **B3**

and a high carbon yielding (65%) resol-type phenolic resin for side-by-side comparisons, as described in the experimental section above. Post-fabrication inspection indicated satisfactory consolidation occurred in the phenolic-derived carbon samples, with a single densification. However, SEM analysis after the phenolic-derived C/C coupons were fractured revealed significant delamination of the carbon fibers from the carbon matrix (Fig. 10a). The results here were obtained without any re-densification cycles for either composite (**B3**-derived or phenolic-derived C/C) or any other composite shown herein. The quality obtained here for the phenolic-derived C/C coupon matches well with

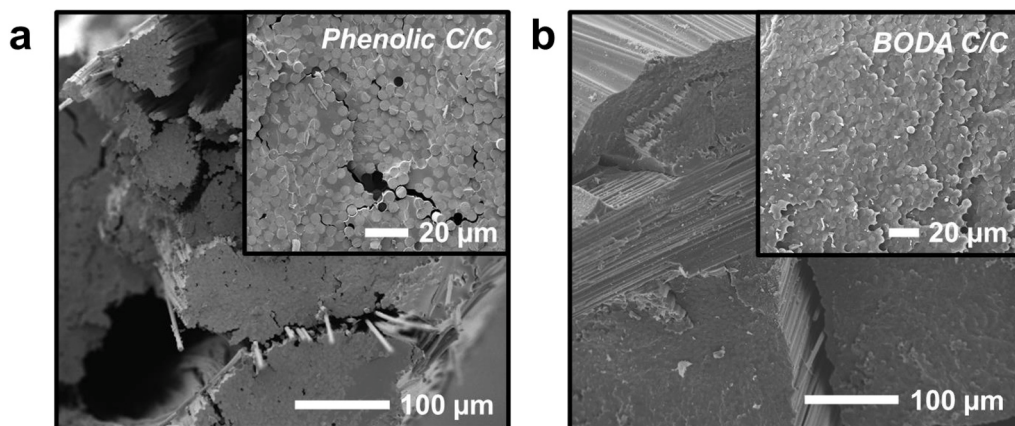


Fig. 10. SEM cross sections of mechanically fractured C/C composites from phenolic-derived (fractured once) (a) and a BODA **B3**-derived carbon matrix (fractured twice) (b). Composite dimensions, fiber content, and both cured and carbonized heating rate (1.5 °C/min to 1000 °C under argon) were constant for each.

recent literature of similarly fabricated composites [49]. In lieu of quantitative mechanical data, the **B3**-derived C/C was fractured in half twice to force extensive delamination between plies and exacerbate other modes of mechanical failure relative to the phenolic-derived C/C coupon (Fig. 10b). However, the **B3**-derived C/C coupons exhibited superior binding properties such as adhesion and interfacial strength that can be seen on both microscopic and macroscopic levels.

The lack of fiber pullout and delamination seen in **B1–B3**-derived C/C composites is quite promising. Other high carbon-yielding arylacetylene resins, for example, show significant delamination and low interlaminar shear strengths (ILSS) [50]. The results presented here for BODA resins are promising because a strong correlation between density and microfeatures of fractured surfaces with mechanical performance is well known [51]. Follow up studies are currently underway to investigate the quantitative mechanical properties of C/C coupons derived from these unformulated BODA-base resins against a baseline of industrial state of the art standards.

4. Conclusions

Three bis-*ortho*-diynyl arene (BODA) monomers (**B1–B3**) were synthesized and studied for use as primary components in matrix resins for carbon/carbon (C/C) composite applications. Each monomer exhibited thermal polymerization, branching, and ultimate network formation via Bergman cyclization. Processing parameters were largely determined by modular spacer and terminal groups which affect properties such as melting behavior, polymerization kinetics, viscosity, and ultimate crystallinity and density of the carbon. Unlike previous poly(arylacetyles), BODA-derived resins can be melt-processed, cured, and pyrolyzed into C/C structures with extremely limited threat of uncatalyzed runaway reactions or hazardous exotherms occurring during the process. Remarkably, melt-processing of **B1–B3** in air is possible without changing the melt, polymerization profile, or resulting carbon significantly. Carbonization of the resulting thermosets gave unprecedented high carbon yields (>80%), which can be enhanced by the presence of oxygen. The stark contrast in chemistry between BODA materials and the current industrial standard (phenolic resins) allows for faster carbonization without unfavorably changing the density and degree of crystallinity in the final carbon. BODA-biphenyl (**B3**) exhibited the highest carbon yields (83%) and final C/C densities of ~1.55 g/cm³ after a nonoxidative pyrolysis at 1000 °C. SEM analysis of fractured BODA-derived C/C coupons demonstrated excellent consolidation, with minimal delamination or carbon-fiber pullout.

Credit authorship contribution statement

Ernesto I. Borrego: Project administration, investigation, data curation, formal analysis, writing-original draft. Sumudu Athukorale: Investigation, data curation, formal analysis. Saidulu Gorla: Methodology, formal analysis. Alison K. Duckworth: Investigation. William W. Johnson: Investigation. Santanu Kundu, Hossein Toghiani, Behzad Farajidizaji, Myles Baker, and Johnathan Rosales: Methodology, resources. Charles U. Pittman, Jr.: Conceptualization, methodology, writing-review and editing. Dennis W. Smith, Jr.: Conceptualization, funding acquisition, supervision, writing-review and editing.

Declaration of competing interest

Ernesto Borrego and Dennis Smith have financial interests in Hand Technologies, LLC. Myles Baker has a financial interest in M4 Engineering. All other authors declare that they have no known competing financial interests or personal relationships that could have appeared to influence the work reported in this paper.

Data availability

No data was used for the research described in the article.

Acknowledgements

The authors would like to acknowledge 1.) the Department of Chemistry at Mississippi State University 2.) Battelle Memorial Institute and NASA Phase I SBIR (80NSSC21C0261) for financial support, in part, for this work. 3.) M⁴ Aerospace Engineering for providing materials and other resources 4.) Dr. Wesley Hoffman, AFRL, Edwards Airforce Base, for assisting with the carbonization. 5.) MSU's Advanced Composites Institute for their donation of T300 carbon fiber.

Appendix A. Supplementary data

Supplementary data to this article can be found online at <https://doi.org/10.1016/j.compositesb.2022.110080>.

References

- [1] Chung DDL. 7 - carbon-matrix composites. Carbon composites. second ed. Butterworth-Heinemann; 2017. p. 387–466.
- [2] White JL, Sheaffer PM. Pitch-based processing of carbon-carbon composites. Carbon 1989;27(5):697–707.
- [3] Brooks JD, Taylor GH. The formation of graphitizing carbons from the liquid phase. Carbon 1965;3(2):185–93.
- [4] Processing of carbon-carbon composites. In: Miracle DB, Donaldson SL, editors. Composites. ASM International; 2001. 0.
- [5] Chung DL. Carbon fiber composites. first ed. Butterworth-Heinemann; 1994.
- [6] Sengh JV, Agboola OD, Li H, Zhu W, Mike Chung TC. Investigation of poly(phenylacetylene) derivatives for carbon precursor with high carbon yield and good solubility. Eur Polym J 2021;147:110289.
- [7] Mathias LJ, Tregre GJ. Synthesis, cure, and composite properties of mixed allyl-propargyl cyclopentadiene resins. J Polym Sci B Polym Phys 1998;36(16):2869–76.
- [8] Wang M-C, Zhao T. Polarylacetylene blends with improved processability and high thermal stability. J Appl Polym Sci 2007;105(5):2939–46.
- [9] Economy J, Jung H, Gogea T. A one-step process for fabrication of carbon-carbon composites. Carbon 1992;30(1):81–5.
- [10] Houck MB, Brown LC, Lambeth RH, Iacono ST. Exploiting the site selectivity of perfluoropyridine for facile access to densified polarylene networks for carbon-rich materials. ACS Macro Lett 2020;9(7):964–8.
- [11] Buchmeiser MR, Muks E, Schowner R, Frank E, Hageroth U, Henzler S, et al. Structure evolution in all-aromatic, poly(p-phenylene-vinylene)-derived carbon fibers. Carbon 2019;144:659–65.
- [12] Sykam K, Harika P, Donempudi S. Flame-retardant, phosphorous-based polyurethane triazoles via solvent-free and catalyst-free azide–alkyne cycloaddition and their cure kinetics. Polym Adv Technol 2021;32(4):1636–53.
- [13] Morgan AB, Tour JM. Synthesis and testing of nonhalogenated alkyne/phosphorus-containing polymer additives: potent condensed-phase flame retardants. J Appl Polym Sci 1999;73(5):707–18.
- [14] Morgan AB, Tour JM. Synthesis and testing of nonhalogenated alkyne-containing flame-retarding polymer additives. Macromolecules 1998;31(9):2857–65.
- [15] Guo K, Li P, Zhu Y, Wang F, Qi H. Thermal curing and degradation behaviour of silicon-containing arylacetylene resins. Polym Degrad Stabil 2016;131:98–105.
- [16] Zhao H-B, Chen L, Yang J-C, Ge X-G, Wang Y-Z. A novel flame-retardant-free copolyester: cross-linking towards self extinguishing and non-dripping. J Mater Chem 2012;22(37):19849–57.
- [17] Connell JW, Smith JG, Hergenrother PM. Composition of and method for making high performance resins for infusion and transfer molding processes, vol. 6. US: NASA; 2000. p. 359. 107 B1.
- [18] Smith JG, Connell JW, Hergenrother PM, Criss JM. Resin transfer moldable phenoxyethynyl containing imide oligomers. J Compos Mater 2002;36(19):2255–65.
- [19] Hay A. Communications- oxidative coupling of acetylenes. J Org Chem 1960;25(7): 1275–6.
- [20] Jones RR, Bergman RG. p-Benzyne. Generation as an intermediate in a thermal isomerization reaction and trapping evidence for the 1,4-benzenediyl structure. J Am Chem Soc 1972;94(2):660–1.
- [21] Bergman RG. Reactive 1,4-dehydroaromatics. Acc Chem Res 1973;6(1):25–31.
- [22] Caldona EB, Borrego EI, Shelar KE, Mukeba KM, Smith DW. Ring-forming polymerization toward perfluorocyclobutyl and ortho-diynylarene-derived materials: from synthesis to practical applications. Materials 2021;14(6):1486.
- [23] Smith DW, Babb DA, Snelgrove RV, Townsend PH, Martin SJ. Polynaphthalene networks from bisphenols. J Am Chem Soc 1998;120(35):9078–9.
- [24] John JA, Tour JM. Synthesis of polyphenylenes and polynaphthalenes by thermolysis of edinylenes and dialkynylbenzenes. J Am Chem Soc 1994;116(11): 5011–2.
- [25] Xiao Y, Hu A. Bergman cyclization in polymer chemistry and material science. Macromol Rapid Commun 2011;32(21):1688–98.

- [26] Shah HV, Brittain ST, Huang Q, Hwu SJ, Whitesides GM, Smith DW. Bis-o-diyenylarene (BODA) derived polynaphthalenes as precursors to glassy carbon microstructures. *Chem Mater* 1999;11(10):2623–5.
- [27] Smith Jr DW, Shah HV, Perera KPU, Perpall MW, Babb DA, Martin SJ. Polyarylene networks via bergman cyclopolymerization of bis-ortho-diyenyl arenes. *Adv Funct Mater* 2007;17(8):1237–46.
- [28] Zengin H, Smith DW. Bis-ortho-diyenylarene polymerization as a route to solid and hollow carbon fibers. *J Mater Sci* 2007;42(12):4344–9.
- [29] Perpall MW, Perera KPU, DiMaio J, Ballato J, Foulger SH, Smith DW. Novel network polymer for templated carbon photonic crystal structures. *Langmuir* 2003;19(18):7153–6.
- [30] Waage SK, Gardner DJ, Elder TJ. The effects of fillers and extenders on the cure properties of phenol-formaldehyde resin as determined by the application of thermal techniques. *J Appl Polym Sci* 1991;42(1):273–8.
- [31] Lee Y-K, Kim D-J, Kim H-J, Hwang T-S, Rafailovich M, Sokolov J. Activation energy and curing behavior of resol- and novolac-type phenolic resins by differential scanning calorimetry and thermogravimetric analysis. *J Appl Polym Sci* 2003;89(10):2589–96.
- [32] Lum R, Wilkins CW, Robbins M, Lyons AM, Jones RP. Thermal analysis of graphite and carbon-phenolic composites by pyrolysis-mass spectrometry. *Carbon* 1983;21(2):111–6.
- [33] Johnson JP, Bringley DA, Wilson EE, Lewis KD, Beck LW, Matzger AJ. Comparison of “polynaphthalenes” prepared by two mechanistically distinct routes. *J Am Chem Soc* 2003;125(48):14708–9.
- [34] Hosomura T, Okamoto H. Effects of pressure carbonization in the C-C composite process. *Mater Sci Eng, A* 1991;143(1):223–9.
- [35] Wong H-W, Peck J, Bonomi RE, Assif J, Panerai F, Reinisch G, et al. Quantitative determination of species production from phenol-formaldehyde resin pyrolysis. *Polym Degrad Stabil* 2015;112:122–31.
- [36] Trick KA, Saliba TE. Mechanisms of the pyrolysis of phenolic resin in a carbon/phenolic composite. *Carbon* 1995;33(11):1509–15.
- [37] Schreiner P R. Cyclic enediynes: relationship between ring size, alkyne carbon distance, and cyclization barrier. *Chem Commun* 1998;(4):483–4.
- [38] Alabugin IV, Manoharan M. Reactant destabilization in the bergman cyclization and rational design of light- and pH-activated enediynes. *J Phys Chem* 2003;107(18):3363–71.
- [39] Ferrari AC, Robertson J. Interpretation of Raman spectra of disordered and amorphous carbon. *Phys Rev B* 2000;61(20):14095–107.
- [40] Perera KPU, Abboud KA, Smith DW, Krawiec M. Three bis-ortho-diyenylarenes (BODA). *Acta Crystallogr C* 2003;59(3):o107–10.
- [41] Ohlhorst CW, Glass DE, Bruce WE, Lindell MC, Vaughn WL, Smith RW, et al. Development of X-43A Mach 10 leading edges. 56th International Astronautical Congress of the International Astronautical Federation, the International Academy of Astronautics, and the International Institute of Space Law.
- [42] Shah HV, Babb DA, Smith DW. Bergman cyclopolymerization kinetics of bis-ortho-diyenylarenes to polynaphthalene networks. A comparison of calorimetric methods. *Polymer* 2000;41(12):4415–22.
- [43] Perera KPU, Shah HV, Foulger SH, Smith DW. Substituent effects on Bergman cyclopolymerization kinetics of bis-ortho-diyenylarene (BODA) monomers by dynamic scanning calorimetry. *Thermochim Acta* 2002;388(1):371–5.
- [44] Any remaining Pd impurities in the monomers will cause a measurable shift from the onset of polymerization, reported here and in previous literature (See ref [23]) due to Pd coordination with the ortho-diene which will also catalyze the Bergman cyclization.
- [45] Bansal RC, Donnet JB. Pyrolytic formation of high-performance carbon fibres. *Compr. Pol. Sci. Suppl.* 1996;16:501–20.
- [46] Laušević Z, Marinković S. Mechanical properties and chemistry of carbonization of Phenol formaldehyde resin. *Carbon* 1986;24(5):575–80.
- [47] Choe CR, Lee KH, Il Yoon B. Effect of processing parameters on the mechanical properties of carbonized phenolic resin. *Carbon* 1992;30(2):247–9.
- [48] Maahs HG, Vaughn WL, Kowbel W. Four advances in carbon-carbon materials technology. In: Proceedings of the fourth national technology transfer conference and exposition. Conference, conference; 1994.
- [49] Yue Z, Vakili A. Activated carbon–carbon composites made of pitch-based carbon fibers and phenolic resin for use of adsorbents. *J Mater Sci* 2017;52(21):12913–21.
- [50] Hergenrother PM. Acetylene-containing precursor polymers. *J Macromol Sci, Part C* 1980;19(1):1–34.
- [51] Tzeng S-S, Chr Y-G. Evolution of microstructure and properties of phenolic resin-based carbon/carbon composites during pyrolysis. *Mater Chem Phys* 2002;73(2):162–9.